A time projection chamber to study two-proton radioactivity

B. Blank [a], L. Audirac [a], G. Canchel [a], F. Delalee [a], C.E. Demonchy [a], J. Giovinazzo [a], L. Hay [a1], P. Hellmuth [a], J. Huikari [a], S. Leblanc [a], S. List [a], C. Marchand [a], I. Matea [a], J.-L. Pedroza [a], J. Pibernat [a], A. Rebii [a], L. Serani [a], F. de Oliveira Santos [b], S. Grévy [b], L. Perrot [b], C. Stodel [b], J.C. Thomas [b], C. Borcea [c], C. Dossat [d], R. de Oliveira [e]

[a] *Centre d'Etudes Nucléaires de Bordeaux Gradignan - Université Bordeaux 1 - UMR 5797 CNRS/IN2P3, Chemin du Solarium, BP 120, 33175 Gradignan Cedex, France*

[b] *Grand Accélérateur National d'Ions Lourds, CEA/DSM - CNRS/IN2P3, Bvd Henri Becquerel, BP 55027, F-14076 CAEN Cedex 5, France*

[c] *NIPNE, P.O. Box MG6, Bucharest-Margurele, Romania*

[d] *DAPNIA, CEA Saclay, F-91191 Gif-sur-Yvette Cedex, France*

[e] *CERN, CH-1211 Geneva 23, Switzerland*

Abstract

Two-proton radioactivity was observed in two experiments in 2002 in the decay of ^{45}Fe. However, these experiments did not allow the observation of the two protons directly. In the present paper, we present a new setup based on the principle of a time-projection chamber which enabled us for the first time to identify directly the two protons. The new setup permits the observation and reconstruction in three dimensions of the traces of the protons. We will discuss the setup and describe its performances.

Key words: two-proton radioactivity, time projection chamber, ASIC electronics
PACS: 29.40.Cs, 29.30.Ep, 29.90.+r

1. Introduction

Two-proton radioactivity was first proposed by Goldanskii [1] in 1960 as a new radioactive decay mode to occur for nuclei for which the emission of one proton is energetically forbidden, but simultaneous two-proton emission from the ground state is allowed due to the nuclear pairing energy. Since then theoretical considerations [2–5] and experimental observations [6–8] allowed to determine ^{45}Fe, ^{48}Ni, ^{54}Zn and other nuclei in this mass region to be the most promising candidates for this new decay mode.

Ground-state two-proton (2p) emission was indeed observed for the first time in experiments at the GANIL LISE3 separator [9] and at the FRS of GSI [10] in the decay of ^{45}Fe. Although these experiments clearly established 2p radioactivity to be the only decay mode which could consistently explain all observational details [9,10], they did not allow the direct identification of the two protons emitted. This is due to the fact that the decay of ^{45}Fe was observed in silicon detectors in which the ions of interest were deeply implanted. Therefore, for the 2p branch, only the total decay energy, the half-life, and the absence of β particles from the concurrent decay by β-delayed charged-particle emission could be firmly established. However, for a more detailed study in particular of the dynamics of 2p radioactivity, more exclusive observables like the individual proton energies and the relative proton-proton angle have to be measured. This necessitates the direct observation of the two protons.

For this purpose, we developed a new detection setup which is based on the principle of a time-projection chamber (TPC). In such a setup, the ions of interest are implanted in a gas volume where the radioactive decay of these isotopes takes place. This chamber then allows correlating in space and in time the implantation and the decay. In addition and due to the relatively long range of the protons in gas as compared to silicon detectors, the charges produced due to the slowing down of the protons can be visualised and the proton traces can be reconstructed in three dimensions. Figure 1 shows schematically such a TPC.

[1] Permanent address: Laboratoire PHLAM, Bâtiment P5 - USTL, F-59655 Villeneuve d'Ascq Cedex, France

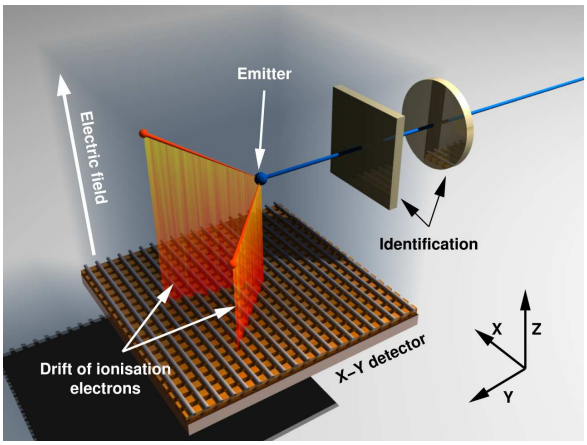

Fig. 1. Schematic representation of a time-projection chamber for 2p events. The isotopes of interest are identified by means of their time of flight and their energy loss with silicon detectors at the entrance of the chamber. The energy of the isotopes is adjusted to stop them in the active volume of the TPC where their decay takes place with a characteristic half-life. The electrons produced by the slowing down of the ions and the protons emitted drift in the electric field of the TPC towards a set of four gas electron multipliers (not shown, 3-10 mm above the 2D detector with a distance of 3-10 mm between two GEMs) where they are amplified. They are finally detected in a two-dimensional detector consisting of x and y strips.

2. Description of the time-projection chamber

2.1. *Geometrical dimensions of the detector*

The TPC is housed in a 60x60x60 cm^3 cubic chamber. The TPC has an active volume of 15x15x6 cm^3. However, due to the electric field configuration, the 15 strips corresponding to 6 mm on either side collect only few electrons and the effective active volume is only about 138x138x60 mm^3. The beam entrance is at a height of about 3 cm above the first gas electron multiplier (GEM), which allows all protons from 2p events to be stopped in the gas before reaching any other material.

Mechanical structures allow α sources to be installed either inside the active volume of the detector or just outside. In particular, a triple-α source is permanently mounted during operation on a circularly moving arm above the drift cathode of the TPC.

2.2. *Electronics of the TPC*

The GEMs are read out by standard electronics. The strips were connected on one end only via flexible printed circuits to connectors which allow passing the signals from the inside of the detector to the outside of the chamber by means of a mother board, on which the 2D detector is mounted. Every second strip of each face of the 2D detector is coupled to ASIC chips, whereas the other half is grouped together in groups of 64 strips and sent to a standard charge-sensitive preamplifier and a shaper. Thus for an active detection surface of 15.36x15.36 cm^2 and a channel to be readout every 400μm, this yields 384 channels for both faces of the 2D detector.

Each of the channels readout individually has an energy and a timing branch. The first channel which fires triggers the whole readout process. The timing of all channels is given with respect to this channel. For the whole detector, 768 energy and 768 time channels have to be treated. This is done by means of the VAT/TAT ASIC chips from IDEAS [11].

The acquisition front end is based on the PXI standard which prepares the signals to be fed into VME modules (CAEN CRAMS). The VME modules are conducted by the GANIL data acquisition and their data are included in the data stream of other VME and VXI modules.

3. Characteristics and performances of the TPC

3.1. *Gas electron multiplier performances*

Gas electron multipliers [12] have been developed in order to amplify the signal produced by ionising particles in gas detectors. The GEMs used in our setup have a total size of 15x15 cm^2 and are subdivided in two halves. They consist of a kapton layer of 50μm thickness covered on both sides with a copper surface (5μm). The hole diameter of the GEMs is 70μm with a distance of 140μm between two hole centres. The GEMs are mounted on an epoxy frame of thickness 2.54 mm.

In our TPC, the electrons produced by the slowing down of the charged particles in the gas drift in the electric field (typically 210 V/cm) of the detector towards the GEMs and the two-dimensional (2D) detector. These electrons are multiplied by a set of four GEMs. The gain of the GEMs depends on the voltage applied across the GEM, the nature of the gas, the gas pressure, and the distance between the GEMs. The charge signal of the upper and lower part of each GEM is coupled out via a capacitor and enables us thus to determine the total energy of a decay event from the different signals of the different GEMs.

Figure 2 shows the energy distribution as determined with a triple-α source (^{239}Pu, ^{241}Am, ^{244}Cm). On all GEMs, the three different α-particle energies can be clearly distinguished and resolutions between 120 and 200 keV are routinely reached.

The GEM gain was measured in a simplified setup. For this purpose, we mounted only two GEMs. Three different gas pressures (500, 750, and 1030 mbar) were used. The gain was defined as the ratio of the signals observed at the lower side of the second versus the first GEM. As shown in figure 3, the gain increases with the voltage applied over the second GEM (the voltage of the first GEM was kept constant).

As will be shown below, the GEMs enable us to obtain sufficiently high gains to detect the low-energy protons from 2p radioactivity events (typical energy of each proton of 550 keV) at the same time as the signals from high-energy

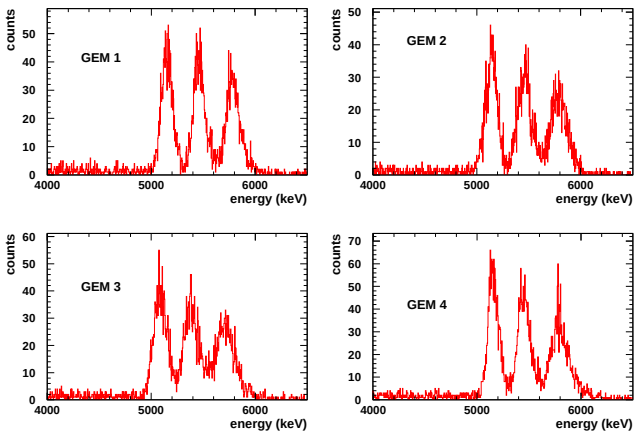

Fig. 2. Energy resolution as obtained with the gas electron multipliers and a triple-α source. For these measurements, the source was mounted just outside the active volume of the TPC. The α particles were emitted parallel to the detection plane and collimated with a collimator of length 3 mm and an opening of 1 mm. The measurement was performed at 500 mbar of P10 (90% Ar - 10% CH_4) with a high voltage of 320 V across the GEMs.

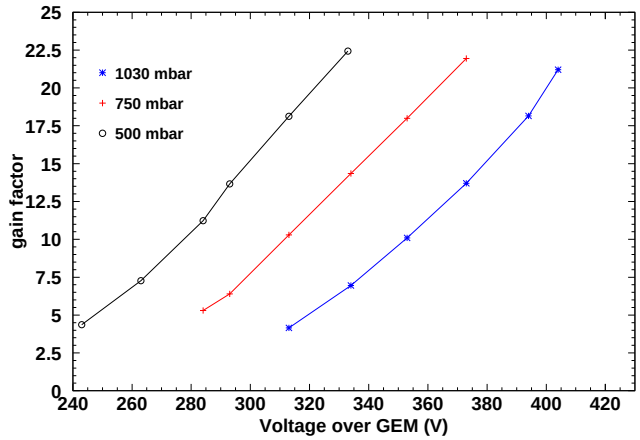

Fig. 3. The figure shows the gains measured for different pressure regimes. The gains were measured with two GEMs and are defined as the ratio between the signals measured on the second GEM and the first GEM. The distance between the GEMs was 10 mm.

events from heavy-ion implantation (typical energy 200-250 MeV). The gains ensure that the charges detected by each strip of the 2D detector are high enough to trigger each individual strip which is necessary for a measurement of the arrival time of the first electrons on each strip (see below).

3.2. *Description and characteristics of the 2D detector*

The 2D detector is a micro-groove detector [13]. The strips on the upper side are orthogonal with respect to the strips on the lower side (see figure 4). The detector consists of a copper coated kapton layer of thickness 50μm. The strips are etched into the copper surface. The top strips have a width of 50μm and a pitch of 100μm. The strips on the top side are connected together two-by-two on both ends. This was meant to increase the gain of the 2D detector when a high voltage is applied between the two strip sides. However, in the present application no high voltage is applied between the two sides (see below).

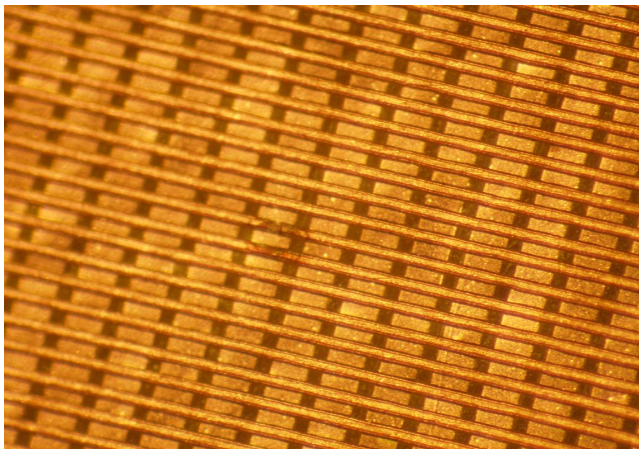

Fig. 4. Photo of the 2D detector composed of a copper-coated kapton foil of thickness 50μm on which the strips have been etched on the upper and lower side. The top strips have a pitch of 100μm and a width of 50μm and are connected on both ends two-by-two. The lower-side strips have a pitch of 200μm and a width of 150μm. The copper thickness on both sides is 5μm.

The lower side of the detector consists of strips with a pitch of 200μm and a width of 150μm. The kapton between the two strip layers is to a large extent removed to allow the charge collection on the top and the bottom side. As the surfaces of the strips are not the same on both sides, a small voltage (typically 10-20 V depending on the high-voltage settings of the TPC) has to be applied to equilibrate the charges collected on both sides [14]. Besides this voltage, the 2D detector is at ground potential.

3.3. *Drift-time characteristics*

In a time projection chamber, the drift-time analysis is used to determine the position of a particle in the direction of the electric field of the chamber. In our purpose, this drift-time analysis serves to analyse the angle of the proton tracks with respect to the detection plane. The charge cloud produced by the energy loss of charged particles drifts towards the detection plane with a constant velocity depending on the nature and the pressure of the gas used and the electric field of the drift zone. The electrons created closer to the detection plane arrive first on this detection plane, whereas electrons produced higher above the two-dimensional detector arrive with some delay. With the known constant drift velocity, the time delay can be transformed into a distance and thus in an angle of the track.

Figure 5 shows the calibration curve determined with α particles entering the detector with a fixed angle. A linear dependence between the entrance angle and the angle determined in the analysis of the drift time is observed. The

angle was determined by a measurement of the arrival time difference of the charge cloud on the different strips. By means of the electron drift velocity in the gas, which depends on the pressure (500 mbar), the drift voltage (about 200V/cm), and the gas type (90% Ar - 10% CH_4), the angle of the α-particle trajectory could be determined. Under online conditions, this correlation is measured with an α source integrated in the drift cathode which can be moved in front of several collimators with well defined angles.

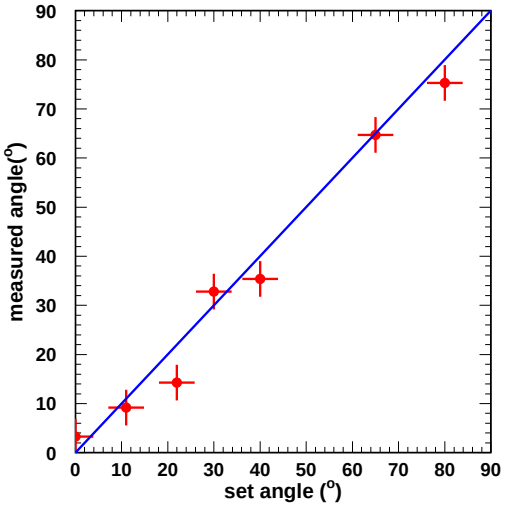

Fig. 5. Drift time calibration as performed with α particles entering the detection volume under fixed angles. With the known drift time which depends on the nature of the gas, its pressure and the drift voltage, the time delay between the strips can be converted into a drift distance and thus into an angle of a trajectory with respect to the detection plane. The angle resolution obtained is 7-8^o.

3.4. *Calibration of the strips*

As mentioned above, the TPC has a total of 768 energy and 768 time channels being readout by ASIC electronics. The signal collected on the different detector strips and the gains of the different ASIC chips can be rather different. Therefore, a precision calibration in energy but also in time is necessary to gain match the different channels.

In the experiment we performed with the TPC (see below), we used two methods to perform this gain matching. First, an offline matching was performed by injecting a pulser signal in the lower side of the last GEM. This signal creates an image charge on the strips in both directions, which allows establishing an energy calibration curve for each strip. The time matching was performed with the same signal by delaying the hold signal for the readout.

This method yields a satisfactory result for the time channels. However, for the energy channels, the signals detected with real events were not as uniform as expected. This might be for example due to slightly varying sizes of the strips and thus varying charge collection. Therefore, we performed a correction, where we used the primary as well as fragment beams which traversed the whole chamber with relatively high energy. This allows assuming that the energy loss per range unit does not change and thus all the strips are supposed to collect the same charge. The different beams yielded different signal heights thus allowing establishing a correction curve for each strip. To calibrate the strips parallel to the beam direction, we rotated the chamber after the experiment and performed a similar scan. Figure 6 shows the signal from an implantation event on the strips perpendicular to the beam direction without calibration, with the pulser calibration and with the additional correction.

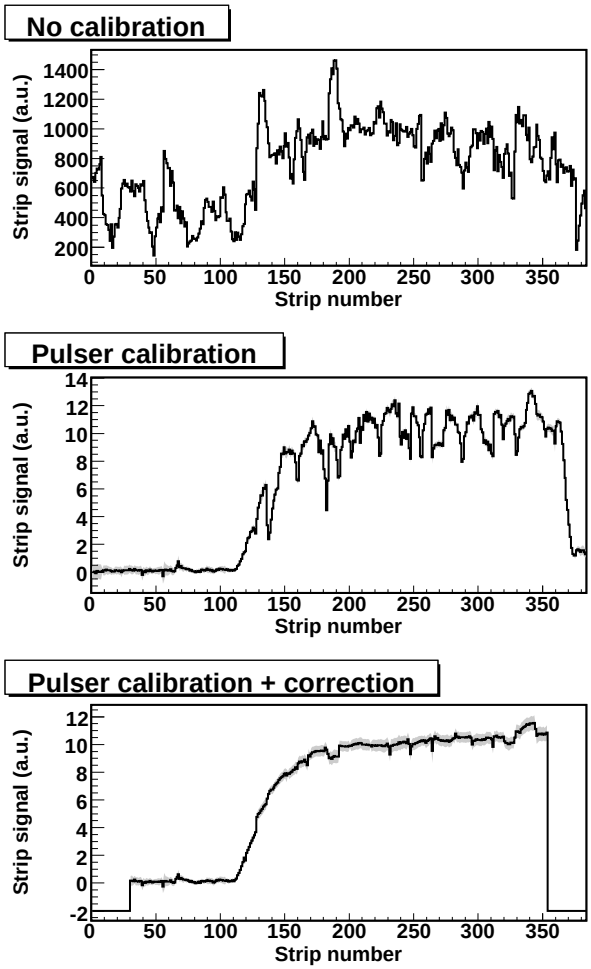

Fig. 6. The signal registered by each strip perpendicular to the beam is shown from an implantation event. The upper spectrum shows the ASIC response without calibration, the center spectrum with the pulser calibration described in the text, and the lower figure with the additional correction by means of the traversing beams. The smoothing procedure is not yet applied for these spectra (see text for details). The shaded area indicates the error bars.

4. Selected online results

After a first online test of the detector at the LISE2000 beam line of GANIL in April 2006, the TPC was used for the

first real data taking in September 2006 [15]. Figure 7 shows the TPC installed at the LISE3 beam line of GANIL. The aim of the experiment was to observe directly the emission of two protons in the decay of ^{45}Fe.

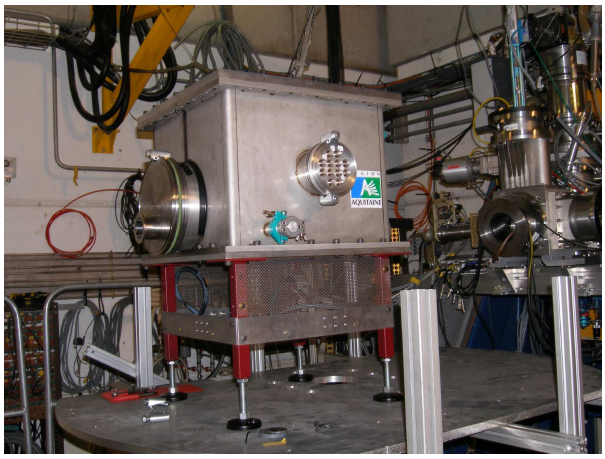

Fig. 7. The TPC installed at the exit of the LISE3 beam line of GANIL.

We obtained implantation and decay events for 10 ^{45}Fe ions. A detailed analysis of these events is under way. The data for ^{45}Fe should allow a rough first comparison between the experimental distributions and theoretical predictions. Figure 8 shows two correlated implantation and decay events for ^{45}Fe.

5. Conclusion and outlook

In the present paper, we described the basic performances as obtained with a time projection chamber built at the Centre d'études nucléaires de Bordeaux-Gradignan. The aim of this TPC is the study of two-proton emission either from nuclear ground states as in the case of ground-state two-proton radioactivity of e.g. ^{45}Fe or from excited states populated by nuclear β decay as e.g. in the case of ^{43}Cr.

The signals produced either by heavy-ion implantation events or by proton emission events are first amplified by a set of four gas electron multipliers and detected by a two-dimensional detector consisting of two orthogonal sets of 768 strips. Every second of the strips is read out by means of ASIC electronics. The third dimension of the events is obtained by time projection of the tracks in the detector gas. This allows visualising events in three dimensions.

The performances described show that the detector is capable to detect 2p events and to determine their basic characteristics such as the energy of the protons and their relative angle. A first experiment performed with this detector demonstrated its performances.

Acknowledgment

We would like to thank the whole GANIL and in particular the LISE staff and the GANIL DAQ group for their help in the preparation phase and during the experiment. This work was supported by the Conseil régional d'Aquitaine and by the European Union via the EURONS/ACTAR contract and through the Human Capital and Mobility programme.

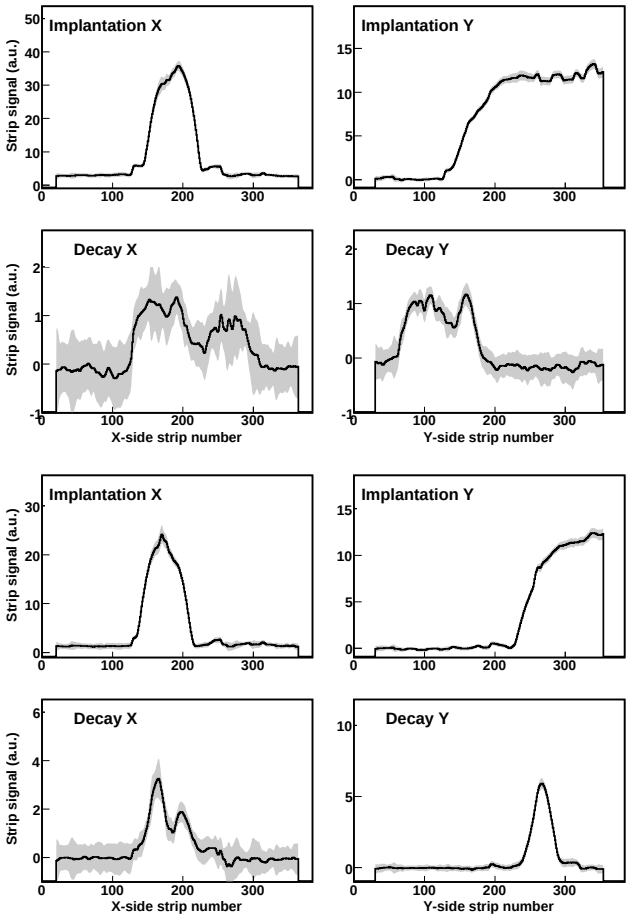

Fig. 8. Two implantation and correlated decay events are shown for ^{45}Fe. The figures show each time the implantation signal on the X and Y strips and the decay signal on the same strips just below. The decay events start where the implantation trajectory ends. In all cases, the tracks of the two protons can be clearly seen.

References

[1] V. I. Goldansky, Nucl. Phys. **19**, 482 (1960).
[2] B. A. Brown, Phys. Rev. C **43**, R1513 (1991).
[3] W. E. Ormand, Phys. Rev. C **53**, 214 (1996).
[4] B. J. Cole, Phys. Rev. C **54**, 1240 (1996).
[5] B. A. Brown, F. C. Barker, and D. J. Millener, Phys. Rev. C **65**, 051309(R) (2002).
[6] B. Blank *et al.*, Phys. Rev. Lett. **77**, 2893 (1996).
[7] B. Blank *et al.*, Phys. Rev. Lett. **84**, 1116 (2000).
[8] J. Giovinazzo *et al.*, Eur. Phys. J. **A11**, 247 (2001).
[9] J. Giovinazzo *et al.*, Phys. Rev. Lett. **89**, 102501 (2002).
[10] M. Pfützner *et al.*, Eur. Phys. J. **A14**, 279 (2002).
[11] www.ideas.no
[12] F. Sauli, Nucl. Instr. Meth. A **386**, 531 (1997).
[13] R. Bellazzini *et al.*, Nucl. Instrum. Meth. **A424**, 444 (1999).
[14] A. Bressan *et al.*, Nucl. Instrum. Meth. **A425**, 254 (1999).
[15] J. Giovinazzo *et al.*, Phys. Rev. Lett. **99**, 102501 (2007).